PROGRESSIVE IMAGE TRANSMISSION OVER A NOISY CHANNEL USING WAVELET TRANSFORM AND CHANNEL OPTIMIZED VECTOR QUANTIZATION

J.L. Pérez-Córdoba[*]

Dpto. Electrónica y Tecn. Computadores
Granada University. 18071 Granada, Spain
E-mail: jlpc@ugr.es

V.G. Ruiz, I. García[†]

Dpto. Arq. de Computadores y Elect.
Almería University. 04120 Almería, Spain
E-mail: vruiz@ual.es, inma@ace.ual.es

ABSTRACT

This paper studies a progressive image transmission technique over waveform channels. The Channel Optimized Vector Quantization codec (COVQ) [1] is applied to the image wavelet coefficients creating a robust progressive image transmission technique that mitigates the effects of a noisy channel on the reconstructed image. In order to evaluate the performance of our proposal, a Gaussian and slow-fading Rayleigh channel model, with several different values of Channel Signal to Noise Ratio (CSNR) were simulated in our experiments. Examples show a significant visual improvement of our application compared to other progressive image transmission techniques.

1. INTRODUCTION

Image compression is an essential tool for storing or transmitting digitized images. For image transmission, progressive image codecs have been shown to be very useful in many different fields [2], because they can produce an increasing quality reconstruction of the original image at the receiver using a minimum amount of the channel capacity. At present, most of the progressive encoding schemes are not suitable to be used over noisy channels. This can be a serious disadvantage in real-time applications, such as image tele-browsing through the Internet and image wireless applications.

This work analizes and evaluates a progressive and error-resilient image codec based on the COVQ technique applied to the wavelet-domain representation of the image that we want to transmit. This wavelet-domain allows us to know which information must be sent first to enable a multiresolution progressive reconstruction of the image at the receiver.

Joint source-channel coding techniques are used to mitigate the effects of channel noise without increasing the bit-rate while protecting against errors. COVQ [1] is one of these techniques. In this work, COVQ is applied to the image wavelet coefficients, thus enabling a procedure for robust progressive image transmission.

This paper is organized as follows. Section 2 briefly describes details of the discrete wavelet transform used in this work. The COVQ technique and its application for coding image wavelet coefficients are discussed in Section 3. In Section 4 performance results are presented and discussed. Finally, Section 5 contains conclusions.

2. THE DISCRETE WAVELET TRANSFORM

The wavelet transform is very suitable to find a compact representation of images because its basis functions are non-stationary, like most of basis signals contained in natural images. The Discrete Wavelet Transform (DWT) is applied to digitized signals. Thus, a signal $s[i],\ i = 0, \cdots, N-1$ (where N is the number of samples) can be decomposed into two signals of half size, one $l[i],\ i = 0, \cdots, \frac{N}{2} - 1$ (the low frequency band) averaging the signal, and the other $h[i],\ i = 0, \cdots, \frac{N}{2} - 1$ (the high frequency band) that contains the information necessary for recovering the original signal $s[\cdot]$ from the average $l[\cdot]$. When fixed point arithmetic is used, the Integer DWT (IDWT) is carried out and the process is completely reversible. Each DWT uses a different low or/and high-pass filter. The IDWT selected to build our progressive codec is the 13/7-T transform [3] which has demonstrated a very high performance for image coding [4]. The 13/7-T transform (also called the (4,4) interpolating transform [3]) is an integer version of the (floating point) 13/7 transform. When transforming finite-length signals, it is also necessary to select some strategies for handling filtering at the signal boundaries. In our implementation the (2,2) and the (1,1) interpolating transforms [3] are used for building the boundary filtering. These filters are applied at a distance of two and one samples, both at the begining and end of the signal.

Since the transforms under consideration are 1-D in na-

[*] In a research visit at the Dpt. of Computer Arch., Almería University

[†] This work was supported by the Ministry of Education of Spain (CICYT TIC99-0361).

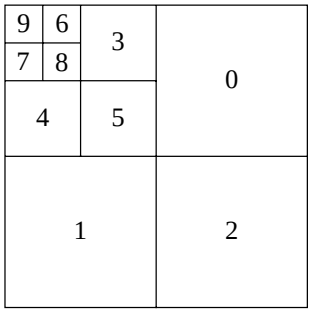

Fig. 1. A dyadic 2D-DWT decomposition of 3 levels.

ture, an image is handled by transforming the rows and columns in succession. After these two steps, the first level of the decomposition is built producing four bands: a low-pass band and three high-pass bands shown in Figure 1 by 0, 1 and 2. When this procedure is applied to the low-pass band n times, we obtain a n-level decomposition.

3. JOINT SOURCE-CHANNEL CODING

In this Section, the fundamentals of the COVQ technique and the necessary optimal conditions are analyzed. To introduce COVQ technique, let us consider a real-valued independent and identically distributed (i.i.d.) source $\mathcal{X} = \{X_i\}_{i=1}^{\infty}$ with probability density function (pdf) $p(x)$. The source is encoded by means of a Vector Quantizer (VQ) whose output is transmitted over a waveform channel. We consider an N vector quantization process with M levels. The COVQ system, as depicted in Figure 2, consists of an encoder mapping γ, a signal selection module and a decoder mapping β. The encoder $\gamma : \mathbb{R}^{\mathrm{N}} \rightarrow \mathcal{I}$, where $\mathcal{I} = \{1, 2, \ldots, M\}$, is described in terms of a partition $\mathcal{S} = \{S_1, S_2, \ldots, S_M\}$ of $\mathbb{R}^{\mathrm{N}}$ according to

$$\gamma(\boldsymbol{x}) = i, \quad \text{if} \quad \boldsymbol{x} \in S_i, \quad i \in \mathcal{I} \tag{1}$$

where $\boldsymbol{x} = (x_1, x_2, \ldots, x_N)$ is a typical source output vector. The signal selection module maps an index i to a signal

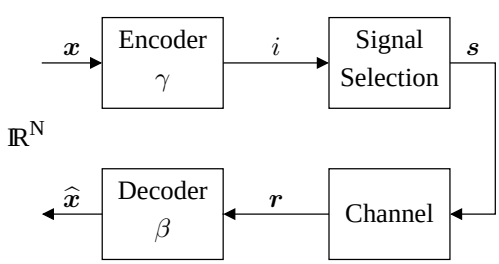

Fig. 2. Block diagram of the COVQ system.

$\boldsymbol{s}$ that is transmitted over the channel. Details of this module can be found in [5].

First, we consider that the channel is an Additive White Gaussian Noise (AWGN) channel. Therefore, the random channel output vector $\boldsymbol{r} = (r_1, r_2, \ldots, r_L)$ is related to the input vector $\boldsymbol{s} = (s_1, s_2, \ldots, s_L)$ through

$$r_l = s_l + n_l, \qquad l = 1, 2, \ldots, L \tag{2}$$

where L is the dimension of the signal constellation and n_l's are i.i.d. zero-mean Gaussian random variables with common variance $\sigma^2 = N_0/2$.

Finally, the decoder β makes an estimate $\widehat{\boldsymbol{x}}$ of the source vector based on the received vector (channel output) $\boldsymbol{r}$. We will restrict our study to hard-decision decoders, that is, the decoder β makes an estimate, $\hat{\boldsymbol{\imath}}$, of the index transmitted, i, represented by the signal $\boldsymbol{s}$, based on the received vector $\boldsymbol{r}$. Given $\hat{\boldsymbol{\imath}}$, the estimate $\widehat{\boldsymbol{x}}$ is selected from a finite reproduction alphabet (codebook) $\mathcal{C} = \{\boldsymbol{c}_1, \boldsymbol{c}_2, \ldots, \boldsymbol{c}_M\}$ that described the decoder through

$$\beta(\hat{\boldsymbol{\imath}}) = \beta\left(\hat{\boldsymbol{\imath}}(\boldsymbol{r})\right) = \boldsymbol{c}_{\hat{\boldsymbol{\imath}}}, \quad \boldsymbol{c}_{\hat{\boldsymbol{\imath}}} \in \mathbb{R}^{\mathrm{N}} \quad \hat{\boldsymbol{\imath}} \in \mathcal{I} \tag{3}$$

The performance of this system is generally measured by the average distortion per sample $\mathcal{D}(\mathcal{S}, \mathcal{C})$ and the encoding rate R. The average distortion is given by

$$\mathcal{D}(\mathcal{S}, \mathcal{C}) = \frac{1}{N} E\left[D\left(\boldsymbol{x}, \beta\left(\hat{\boldsymbol{\imath}}(\boldsymbol{r})\right)\right)\right] \tag{4}$$

where $E[\cdot]$ means the expectation value and $D(\boldsymbol{x}, \boldsymbol{y}) = \|\boldsymbol{x} - \boldsymbol{y}\|^2$. The encoding rate is given by

$$R = \frac{1}{N} \log_2 M \ \text{ bits/sample} \tag{5}$$

and the average distortion by ([1])

$$\mathcal{D}(\mathcal{S}, \mathcal{C}) = \frac{1}{N} \sum_{i=1}^{M} \int_{S_i} p(\boldsymbol{x}) \left\{ \sum_{\hat{\boldsymbol{\imath}}=1}^{M} P(\hat{\boldsymbol{\imath}}|i) D(\boldsymbol{x}, \boldsymbol{c}_{\hat{\boldsymbol{\imath}}}) \right\} \mathrm{d}\boldsymbol{x} \tag{6}$$

where $p(\boldsymbol{x}) = \prod_{n=1}^{N} p(x_n)$ is the N-dimensional source pdf and $P(\cdot|\cdot)$ are transition probabilities for an AWGN channel.

For a given source, a given channel, a fixed dimension N and a fixed codebook size M, we wish to minimize $\mathcal{D}(\mathcal{S}, \mathcal{C})$ by a proper choice of $\mathcal{S}$ and $\mathcal{C}$.

As in [1], it becomes clear that for a fixed $\mathcal{C}$, the optimum partition $\mathcal{S}^* = \{S_1^*, S_2^*, \ldots, S_M^*\}$ is given by

$$\begin{aligned} S_i^* \quad = \quad & \Bigg\{ \boldsymbol{x} \ : \ \sum_{\hat{\boldsymbol{\imath}}=1}^{M} P(\hat{\boldsymbol{\imath}}|i) D(\boldsymbol{x}, \boldsymbol{c}_{\hat{\boldsymbol{\imath}}}) \\ & \leq \ \sum_{\hat{\boldsymbol{\imath}}=1}^{M} P(\hat{\boldsymbol{\imath}}|j) D(\boldsymbol{x}, \boldsymbol{c}_{\hat{\boldsymbol{\imath}}}) \Bigg\} \quad i, j \in \mathcal{I} \end{aligned} \tag{7}$$

Similarly, the optimal codebook $\mathcal{C}^* = \{\boldsymbol{c}_1^*, \boldsymbol{c}_2^*, \ldots, \boldsymbol{c}_M^*\}$ for a fixed partition is given by [1]

$$\boldsymbol{c}_{\hat{\boldsymbol{\imath}}}^* = \frac{\sum_{i=1}^{M} P(\hat{\boldsymbol{\imath}}|i) \int_{S_i} \boldsymbol{x} p(\boldsymbol{x}) \mathrm{d}\boldsymbol{x}}{\sum_{i=1}^{M} P(\hat{\boldsymbol{\imath}}|i) \int_{S_i} p(\boldsymbol{x}) \mathrm{d}\boldsymbol{x}}, \quad \hat{\boldsymbol{\imath}} \in \mathcal{I} \tag{8}$$

A successive application of (7) and (8) produces a sequence of encoder-decoder pairs which converges to a local minimum as the LBG [6] algorithm does.

Assuming that the channel is a slow-fading Rayleigh channel, optimum expressions (7) and (8) are still valid with the only difference that transition probabilities are, in this case, functions of the received SNR, ν, (the channel SNR, CSNR). Therefore, to compute the average distortion of the system we have to use average values of transition probabilities over all values of the received SNR. In other words, we have to compute

$$\overline{P(j|i)} = \int_0^\infty P(j|i) p(\nu) \mathrm{d}\nu \quad i, j \in \mathcal{I} \tag{9}$$

where $p(\nu)$ is the pdf of ν.

3.1. COVQ applied to image coding

In this work, we study the performance of implementing COVQ applied to the coding of image wavelet coefficients when the transmission is over a waveform channel. To do that, we consider a 3 level decomposition of the 13/7-T transform. Table 1 shows codebook size (bit allocation) to the different sub-bands. The resulting compression rate is 0.86 bpp.

There is a noticiable loss in coded image quality due to the lowest sub-band (number 9) wavelet coeficients need for an accurate coding. We have implemented the COVQ technique in all sub-bands except in number 9, where a channel optimized scalar quantization technique [7] is applied. We note this experiment as COSVQ. Table 1 also shows bit allocation of the COSVQ experiment. The resulting compression rate is 0.92 bpp.

For comparison purposes, we present performance results of implementing the LBG algorithm under the same analysis characteristics.

4. RESULTS AND DISCUSSION

In this Section performance evaluations of the considered quantization techniques for several CSNR values are reported. Peak Signal to Noise Ratio (PSNR) is used as the performance measure. For codebook design four CSNR (21, 12, 6 and 0 dB) have been considered. Performance results are obtained simulating the channel models at CSNR values of 21, 12, 6 and 0 dB and using GMSK modulation.

Table 2 shows results for the PSNR. Rows marked as COSVQ-X give performance results for COSVQ technique where quantization codebooks are trained at a CSNR of X dB. Rows marked as COVQ-X provide the corresponding performance results for COVQ technique for the considered CSNR of training. Row marked as VQ gives performance results for the application of LBG algorithm and S+VQ gives performance results for LBG algorithm applied to all sub-bands except number 9.

Table 1. Codebook sizes for the different experiments and sub-bands (see Figure 1 for sub-band nomenclature).

COVQ		COSVQ	
Sub-band number	Codebook size	Sub-band number	Codebook size
0-2	8	0-2	8
3-5	16	3-5	16
6-9	128	6-8	128
		9	64

Table 2. PSNR results for the several different experiments and several values of CSNR: (a) an AWGN Channel; (b) Slow-fading Rayleigh Channel.

	CSNR (dB)			
	21	12	6	0
COSVQ-21	**30.58**	**30.58**	23.81	16.74
COSVQ-12	**30.58**	**30.58**	23.81	16.73
COSVQ-6	30.14	30.14	**27.71**	16.74
COSVQ-0	25.58	25.58	25.25	**22.06**
COVQ-21	26.88	26.88	22.57	15.88
COVQ-12	26.86	26.86	22.56	16.00
COVQ-6	26.18	26.18	24.29	18.17
COVQ-0	23.80	23.80	23.27	20.08
S+VQ	30.28	30.27	23.64	16.25
VQ	26.32	26.32	22.36	15.20

(a) AWGN Channel.

	CSNR (dB)			
	21	12	6	0
COSVQ-21	**29.52**	25.38	23.69	17.67
COSVQ-12	29.40	26.46	21.99	18.79
COSVQ-6	27.34	**26.53**	23.69	20.58
COSVQ-0	26.54	25.68	**23.77**	**21.37**
S+VQ	27.94	21.91	17.76	15.54

(b) Slow-fading Rayleigh Channel.

Table 2 shows that the COSVQ technique gives the best performance results for all considered CSNR. As it was commented, COVQ technique provides poor performance results due to a low accuracy in quantizing wavelet coefficient of sub-band number 9. It is worth noting that COSVQ is better than COVQ, S+VQ and VQ techniques in terms of an objective performance measure (PSNR) and in subjective terms, as it can be seen in Figure 3 that shows an example of the progressive transmission of Lena coded with COSVQ-6 and transmitted over an AWGN Channel at a CSNR of 6 dB. The differences in performance between COSVQ and the others techniques are larger for a slow-fading Rayleigh Channel, in which the bit error rates are bigger.

5. SUMMARY

We have studied joint source-channel coding techniques, COSVQ and COVQ, applied to the coding of image wavelet coefficients. Simulations have shown that it is possible to achieve a good quality of the decompressed image at the receiver when transmitting over a noisy channel, compared to other techniques. It is also shown that it is a suitable technique for progressive transmission over a noisy channel.

6. REFERENCES

[1] N. Farvardin and V.A. Vaishampayan, "On the Performance and Complexity of Channel-Optimized Quantizers," *IEEE Trans. on Information Theory*, vol. 37, no. 1, pp. 155–160, Jan. 1991.

[2] V.G. Ruiz, J.J. Fernández, M.F. López, and I. García, "Progressive Image Transmission in Telemicroscopy: A Quantitative Approach for Electron Microscopy Images of Biological Specimens," *Real Time Imaging (to appear)*, April 2002.

[3] A.R. Calderbank, I. Daubechies, W. Sweldens, and B.-L. Yeo, "Lossless Image Compression Using Integer to Integer Wavelet Transforms," in *Int. Conf. Image Processing (ICIP)*. Oct. 1997, vol. 1, pp. 596–599, IEEE Press.

[4] M.D. Adams and F. Kossentini, "Reversible Integer-to-Integer Wavelet Transforms for Image Compression: Performance Evaluation and Analysis," *IEEE Trans. Image Process.*, vol. 9, no. 6, pp. 1010–1024, 2000.

[5] J.L. Pérez-Córdoba, A.J. Rubio, J.M. López-Soler, and M.C. Benítez, "Hard-Decision in COVQ Over Waveform Channels," in *IEEE Data Compression Conference*, J.A. Storer and M. Cohn, Eds., Mar. 2000, pp. 53–62.

Fig. 3. Examples of progressive transmissions (AWGN Channel; CSNR = 6 dB).

[6] Y. Linde, A. Buzo, and R.M. Gray, "An Algorithm for Vector Quantizer Design," *IEEE Trans. on Communications*, vol. 28, pp. 84–95, Jan. 1980.

[7] N. Farvardin and V.A. Vaishampayan, "Optimal Quantizer Design for Noisy Channels: An Approach to Combined Source-Channel Coding," *IEEE Trans. on Information Theory*, vol. 33, no. 6, pp. 827–838, Nov. 1987.